

On the Role of Color Temperature and Color Rendering Index of White-Light LEDs on the Theoretical Efficiency Limit of Indoor Photovoltaics

Aditi Sharma¹, Alexander A. Guaman¹, Jason A. Röhr^{1,*}

¹General Engineering, Tandon School of Engineering, New York University, Brooklyn, 11201 New York, United States of America

*jasonrohr@nyu.edu

ABSTRACT

As the Internet of Things (IoT) continues to grow, the demand for sustainable indoor power sources is increasing. Indoor photovoltaics (IPVs), which are currently in development, present a renewable solution but need to be designed to match specific light sources. While previous studies have emphasized the role of white-light LED color temperature (CT) in determining IPV efficiency and optimum bandgap energy, the role of color rendering index (CRI) remains less understood. In this study, we employ detailed-balance calculations to assess the theoretical maximum efficiency and optimal bandgap energies of IPVs under commercial white-light LED irradiance varying in both CT (2200 K to 6500 K) and CRI (70, 80, and 90). Our results confirm that lower CTs indeed yield higher efficiencies and lower optimal bandgaps. However, contrary to prior assumptions that CRI has negligible impact on IPV material choice and performance, we demonstrate that high-CRI LEDs necessitate the use of materials with significantly lower bandgap energies for optimum efficiency. We also evaluate the performance of various IPVs at fixed bandgaps, revealing that while optimal IPV performance is achieved with wide-bandgap materials under lower CRI lighting, mature technologies like silicon and CdTe benefit from high-CRI illumination. These findings underscore the need to consider both CT and CRI in the design and evaluation of IPVs for indoor IoT applications.

The goal of the Internet of Things (IoT) is to create a network of interconnected devices that can collect and exchange data without human intervention, thereby automating tasks and improving decision-making via data analysis, with the ultimate hope of enhancing efficiency and productivity across various industries and aspects of daily life. However, wide-spread implementation of the IoT faces a challenge in sustainably powering a rapidly growing number of devices—with an estimated 40 billion integrated devices by 2027.^{1,2} While many IoT devices currently consume only minimal power, ranging from nW to mW, the explosive growth of IoT technologies underscores the need for utilizing sustainable energy sources. Indoor photovoltaics (IPVs) provide a promising, renewable alternative, offering the potential to reduce the environmental impact associated with battery replacement and disposal.¹⁻³ While IPVs have powered rudimentary indoor devices for decades, for example pocket calculators, and even though there is a drive towards reducing the power needed for IoT infrastructure, the growing number of devices are calling for efficient IPVs to be developed. Moreover, as emission profiles vary between

indoor light sources, including those of commercial white-light LEDs, and since the choice of light source determines what material should be chosen as the photo-active component, there is not only a need to develop efficient IPVs, but also a need to understand how to optimize IPVs to match specific indoor lighting environments.

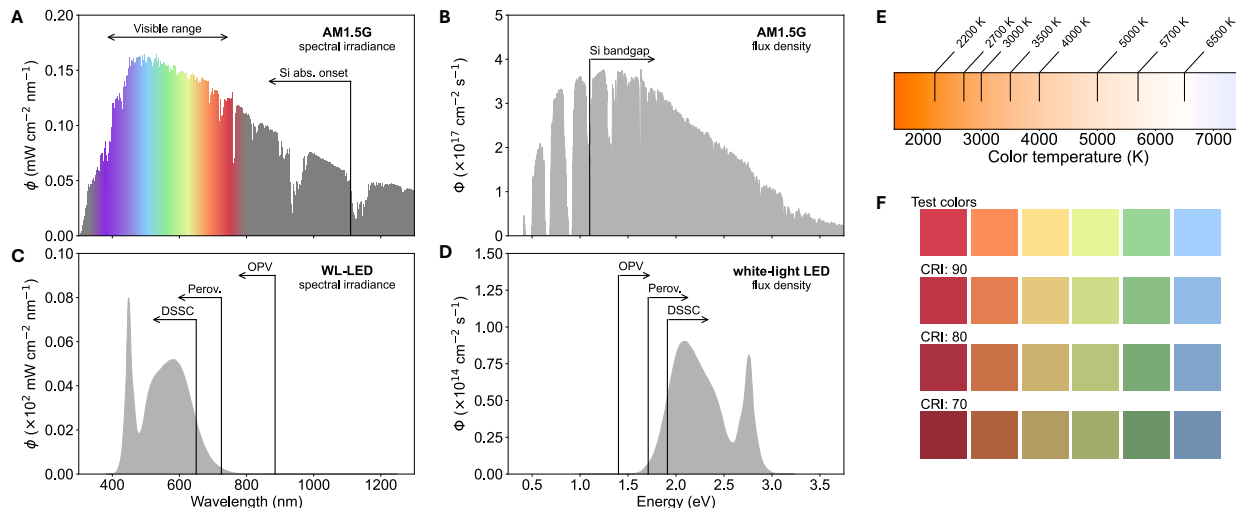


Figure 1 – **A**, AM1.5G solar irradiance, indicating the visible range of the solar spectrum and the absorption onset for crystalline silicon. **B**, Corresponding photon flux density of the AM1.5G spectrum and bandgap edge of crystalline silicon. **C**, Irradiance ($a = 0.1$) of a typical white-light LED (here a Cree J Series LED with CT: 5000 K and CRI: 80) and absorption onsets of DSSC, perovskite, and OPV materials used in record-efficiency IPVs. **D**, Corresponding photon flux density and bandgap values for DSSC, perovskites, and OPV materials. **E**, Visualization of CT, highlighting the specific values of the employed LEDs. **F**, Visualization of CRI, showing how certain test colors vary with decreasing CRI.

The spectral irradiance spectrum of the Sun spans a wide range of wavelengths, from ultraviolet (UV) to the infrared (IR), with most of its irradiance concentrated in the visible and near-IR regions (**Fig. 1A,B**). Crystalline silicon (c-Si) solar cells, with a bandgap of ~ 1.1 eV (**Fig. 1B**), corresponding to an absorption onset at a wavelength of approximately ~ 1110 nm (**Fig. 1A**), are efficient at converting sunlight into electricity as its (albeit indirect) bandgap is near the theoretical optimum.^{4,5} This, along with the abundance and well-established manufacturing processes of Si, makes it a leading material for outdoor photovoltaic applications. In contrast, indoor lighting, such as white-light LEDs (**Fig. 1C,D**), not only emits at lower intensities but also within a much narrower spectral range (often solely in the visible). This shifts the calculated theoretical maximum to much larger values of ~ 1.8 to ~ 2.0 eV.^{6,7} As c-Si solar cells rely heavily on absorption in the IR (**Fig. 1A,B**), they are therefore less efficient in typical indoor environments. Researchers are therefore actively exploring alternative technologies for powering indoor IoT applications. Perovskite,^{8,9} organic,^{10,11} and dye-sensitized solar cells^{12,13} have optical gaps (and therefore absorption onsets) that can be chosen to match emission profiles of indoor light sources (**Fig. 1C,D**), and have shown great promise for IPV applications with measured indoor power-conversion efficiencies ranging from 30 to 45%. Despite these successes, IPV efficiencies are still far from their calculated theoretical maxima.⁶

To lay the groundwork for understanding the theoretical efficiency limits and optimum bandgap values for IPVs, Freunek *et al.* used detailed-balance calculations, employing irradiance spectra from a set of common indoor light sources.⁶ They found that the device efficiency was, unsurprisingly, highly dependent on how well the bandgap of the active material matches the emission spectrum of the light sources. In fact, they observed that the optimum bandgap for solar cells illuminated by white-light LEDs are in the range of 1.9 to 2.0 eV, with theoretical efficiencies approaching 60%. White-light LED emission spectra are characterized by their color temperature (CT) and color rendering index (CRI). CT refers to the perceived warmth or coolness of a given light source (measured in K), where a lower temperature indicates a warmer, red light and a higher temperature indicates a cooler, blue light (**Fig. 1E**). CRI, which is given on a scale of 0 to 100, is a measure that indicates how accurately a given light source displays colors of an object compared to natural daylight (**Fig. 1F**). A greater CRI often comes at a higher price point and is achieved by widening the irradiance spectrum, typically by either incorporating additional mono-chromatic LEDs into the device or by including phosphors. While emphasis is often put on the CT of the light source within the IPV literature, that is typically not the case for CRI. Ho *et al.* used a similar approach to that of Freunek *et al.*, revealing, among other things, the significance of CT in influencing IPV performance; colder, blue light generally resulting in lower theoretical efficiency at higher bandgap values.⁷ Using an approach of forming white-light emission from a superposition of monochromatic LEDs, Zheng *et al.* found that while CT of white-light LEDs indeed is a dominant factor controlling IPV efficiency, with the power conversion efficiency decreasing as color temperature increases, they observed that CRI affects IPV performance to a lesser extent regardless of the CT values.¹⁴

Building on these past reports, we here investigate the theoretical maximum efficiencies and optimum bandgaps of IPVs modeled as if illuminated by a range of commercial white-light LEDs with varying CT (2200 K to 6500 K) and CRI (70, 80, and 90), covering the typical range sold by manufacturers. Our analysis confirms that both the maximum efficiency and optimum bandgap value of the solar cell varies with CT of the LEDs. Contrary to previous reports, our calculations reveal that choice of LED CRI is significant, with IPVs illuminated by 90 CRI white-light LEDs having slightly less maximum theoretical efficiency at significantly lower optimal bandgap values across all CT values investigated due to the broader emission spectral profile. However, we show that technologies such as c-Si and CdTe benefit from illumination with high-CRI light. This indicates the need for device engineers to account for a broader range of LED characteristics, beyond CT alone, when designing and characterizing IPVs.

Similar to the approaches outlined above,^{6,7,14} we utilized a detailed-balance model to calculate the maximum power-conversion efficiency of IPVs when illuminated by a range of commercial white-light LEDs with varying CT and CRI values. We obtained the LED irradiance spectra as a function of wavelength, $\varphi_0(\lambda)$, directly from online data

sheets provided by Samsung (LM301Z+ and LH502D), Cree (X Lamp and J Series, and Lumileds (LUXEON 3030 HE and LUXEON 5050). Mean values and standard deviation of the LED irradiance spectra at 4000 K, 5000 K, and 6500 K are shown for CRI values of 70, 80, and 90 in **Fig. 2A-C**, respectively. Irradiance spectra of all the individual LEDs investigated herein are shown in the **Supplementary Material** (Fig. S1-3). A total of 121 irradiance spectra were used within our calculations.

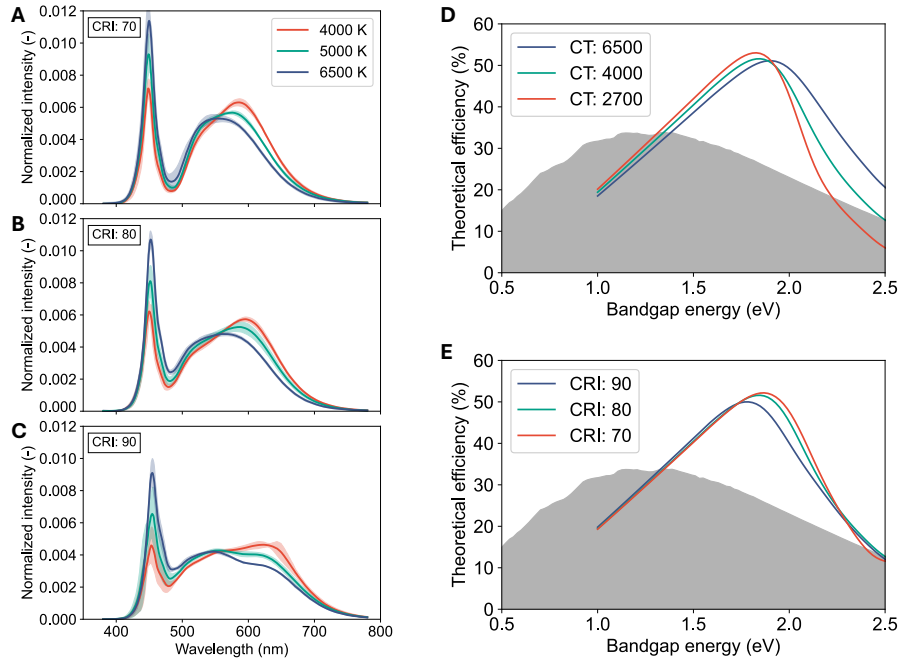


Figure 2 – Averaged, normalized emission spectra of white-light LEDs with CT of 4000 K, 5000 K, and 6500 K for different value of CRI: **A**, 70, **B**, 80, and **C**, 90. **D**, Maximum theoretical efficiency as a function of bandgap energy for a solar cell illuminated under either standard AM1.5G conditions (gray) or illuminated by a LEDs at different CTs and a CRI of 80. **E**, Maximum theoretical efficiency of a solar cell illuminated by LEDs with different CRI values and CT of 4000 K.

While it has been pointed out that IPVs should ideally be characterized on the basis of lighting luminance (in lux) rather than power density (in mW cm^{-2}),² in order to make a simple, direct comparison between all the LED spectra utilized within the present study, and to offer an easy relationship between power output and efficiency of the IPVs, we set all LEDs to have irradiance and therefore power density of comparable magnitude. To do this, each irradiance spectrum was first normalized to have an area of unity,

$$\varphi_{\text{norm}}(\lambda) = \frac{\varphi_0(\lambda)}{\int_{\lambda_1}^{\lambda_2} \varphi_0(\lambda) d\lambda} \quad (1)$$

which allows us to set the irradiance of each LED to a set magnitude, via a dimensionless factor, a ,

$$\varphi(\lambda) = a\varphi_{\text{norm}}(\lambda). \quad (2)$$

This ensures that our comparisons isolate the spectral shape (CRI and CT) at fixed and comparable total irradiance. White-light LEDs used for indoor lighting typically emit light at low power densities (from $\sim 0.1 \text{ mW cm}^{-2}$ to $\sim 10 \text{ mW cm}^{-2}$) as compared to sunlight (100 mW cm^{-2} for AM1.5G). For the present study, values for a that match that of typical irradiance of indoor white-light LEDs were therefore chosen, i.e., $a = 0.1$ to 10 .

The efficiency of a solar cell is determined by the ratio of output to input power (or power density),

$$\eta = \frac{p_{\text{out}}}{p_{\text{in}}} \quad (3)$$

While p_{out} will be determined from the detailed-balance model, p_{in} for a given LED spectrum can be determined by integrating the chosen irradiance spectrum across all relevant wavelengths,

$$p_{\text{in}} = \int_{\lambda_1}^{\lambda_2} \varphi(\lambda) d\lambda. \quad (4)$$

To calculate p_{out} , we begin by converting the spectral irradiance into photon flux density, $\Phi(E)$ via a Jacobian transformation,

$$\Phi(E) = \varphi(\lambda) \frac{hc}{E^2} \quad (5)$$

where h is Planck's constant, c is the speed of light in vacuum, and E is energy. If each photon with energy exceeding the bandgap, E_g , of the active semiconductor contributes to a single electron-hole pair, the photocurrent density can be defined via the photon flux density as,

$$J_{\text{ph}}(E_g) = q \int_{E_g}^{E_2} \frac{\Phi(E)}{E} dE \quad (6)$$

where q is the elementary charge. Radiative recombination is inevitable for any warm body. Assuming ideal diode behaviour, and that the Fermi-level splitting is equal to the external voltage, V , the lowest possible radiative recombination current density is defined as,

$$J_{\text{rec}}(V, E_g, T_c) = \frac{2\pi q}{h^3 c^2} \int_{E_g}^{E_2} \frac{E^2}{\exp\left(\frac{E - qV}{k_B T_c}\right) - 1} dE \quad (7)$$

where T_c is the solar cell temperature (which is assumed to be 300 K for all calculations). Finally, the total current density, J_{tot} , is due to the difference between the photocurrent and the recombination current,

$$J_{\text{tot}}(V, E_g, T_c) = J_{\text{ph}}(E_g) - J_{\text{rec}}(V, E_g, T_c) \quad (8)$$

and p_{out} is now given by the maximum of the product of the current density of the illuminated cell and the applied voltage,

$$p_{\text{out}} = \max(|J_{\text{tot}}V|) \quad (9)$$

Comparisons between the detailed-balance limit assuming standard AM1.5G illumination (the well-known Shockley-Queisser limit) with equivalent calculations using indoor LEDs, is shown in **Fig. 2D,E** highlighting that the maximum efficiency for IPVs approaches 60% and is achieved with much larger bandgap values for the active semiconductor.

The averages of the calculated theoretical maximum efficiencies and optimal bandgap energies are shown in **Fig. 3A-F**; the observed standard deviations within these calculations arise from the deviations in irradiance between the various, investigated LED spectra (**Fig. 2A-C**). As reported elsewhere, IPVs illuminated by LEDs with lower CT yield the highest theoretical maximum power-conversion efficiencies at the lowest optimal bandgaps.^{7,14} The same trend is observed herein for all investigated LEDs regardless of the magnitude of the irradiance (**Fig. 3A,C,E**). Although optimal bandgap values remain relatively unchanged across irradiance levels, calculated efficiencies increase with irradiance, ranging from ~51% (CRI: 90, CT: 6500 K) to ~56% (CRI: 70, CT: 2000 K) for $a = 1$ (**Fig. 3A**) and from ~56% (CRI: 90, CT: 6500 K) to ~61% (CRI: 70, CT: 2000 K) for $a = 10$ (**Fig. 3E**).

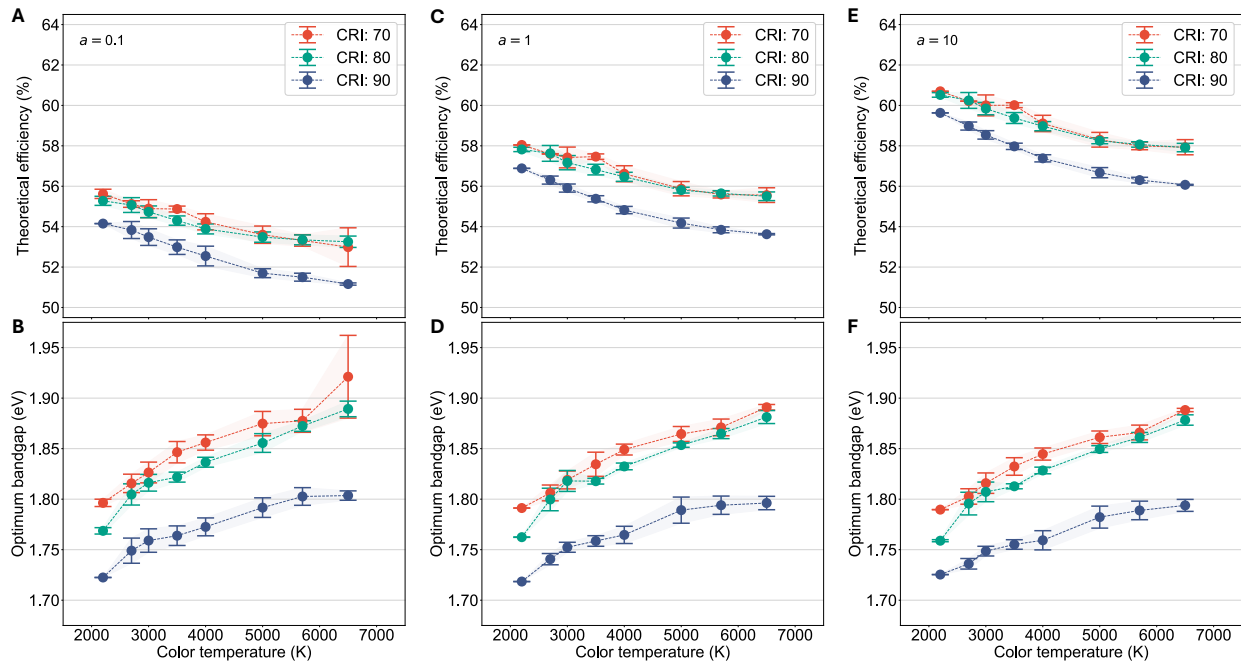


Figure 3 - A, Averages and standard deviations of calculated theoretical maximum efficiencies of IPVs illuminated by white-light LEDs ($a = 0.1$) with different CT values (ranging from 2200 K to 6500 K) and CRI values (70, 80, and 90). **B,** Corresponding averages of calculated optimum bandgap energies resulting in maximum theoretical efficiency. **C,D,** Similar calculations but with $a = 1$. **E, F,** Calculations for $a = 10$.

No significant differences are observed in the calculated results between LEDs with CRI values of 70 and 80, regardless of the magnitude of the irradiance (**Fig. 3A-F**), echoing the previous reports that the choice of CRI of the LEDs do not have a significant impact on the IPVs they are illuminating. However, a deviation is observed for IPVs illuminated by an LED with CRI of 90 yielding not only slightly lower efficiencies ($\sim 54\%$ at 2200 K to $\sim 51\%$ at 6500 K for $a = 0.1$), but yielding said efficiencies at significantly lower bandgap energies (~ 1.72 to ~ 1.80 eV as compared to ~ 1.76 eV to ~ 1.92 eV for 70 and 80 CRI LEDs). This is not entirely surprising, as LEDs with CRI of 90 have broader emission profiles, with higher emission intensities at larger wavelengths as compared to spectra with CRI of 70 and 80 (**Fig. 2A**). So, while it was previously reported that CRI has a lesser impact on solar cell device efficiency,¹⁴ we here show that once the spectral profile of the LED becomes more complex at a CRI of 90, lower bandgap materials must be utilized for optimal performance.

Finally, we investigate whether certain types of solar cells, spanning both mature and next-generation cells, are affected by the choice of LED CT and CRI. To do this, we calculate and compare the maximum theoretical efficiency at set values of the bandgap (**Fig. 4A-D**): 1.1 eV (corresponding to c-Si), 1.3 eV (corresponding to GaAs) 1.5 eV (corresponding to CIGS, CdTe, and record perovskite cells), and 1.8 eV (corresponding to a-Si:H and various next-generation cells). The magnitude of the spectral irradiance was set to a constant value ($a = 0.1$) to allow for a direct comparison.

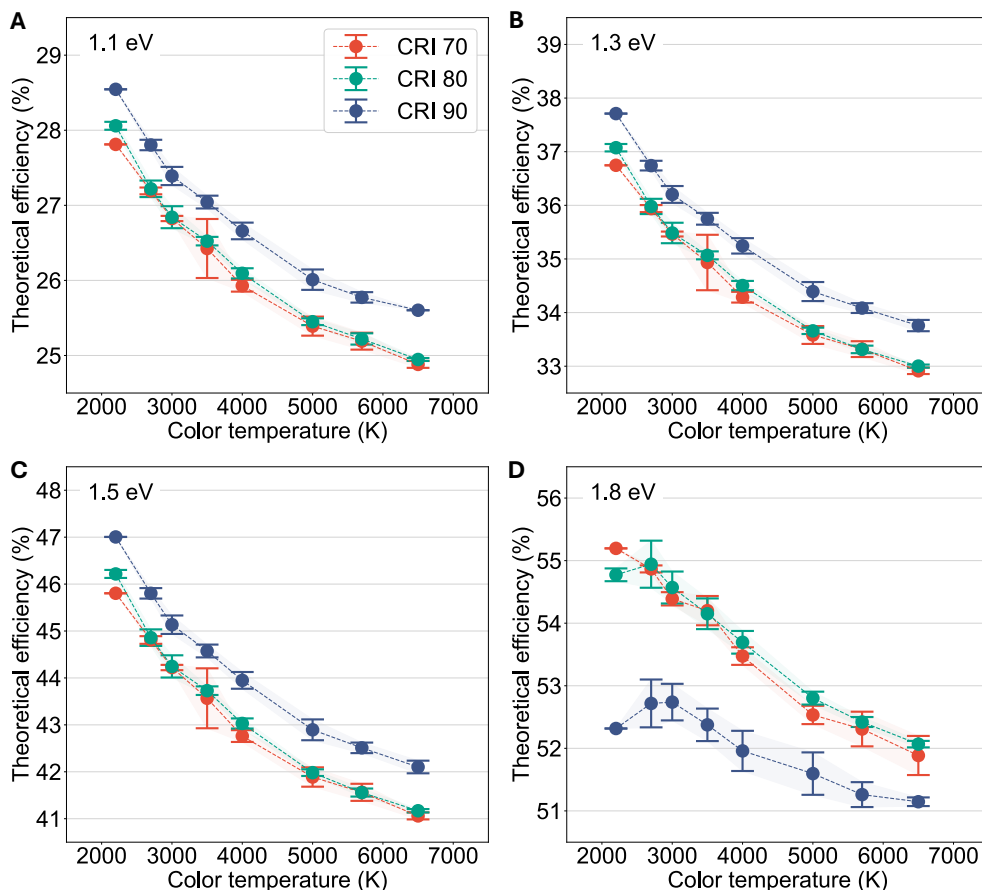


Figure 4 – Mean theoretical maximum efficiency and standard deviation as a function of WL-LED color temperature for solar cells with bandgap values of **A**, 1.1 eV, **B**, 1.3 eV, **C**, 1.5 eV, and **D**, 1.8 eV when illuminated by WL-LEDs ($\alpha = 0.1$) with different CRI values (70, 80, and 90).

As observed in **Fig. 4A-C**, while the magnitude of the theoretical efficiency increases with larger bandgap values as they approach the theoretical optimum, no significant differences in IPV efficiency are, again, observed between using LEDs with CRI of 70 and 80. However, for IPVs with bandgaps between 1.1 to 1.5 eV, the highest theoretical efficiencies are observed for 90 CRI LEDs due to the extended irradiance spectrum into the red. Therefore, if commercial cells such as c-Si or CdTe are employed as IPVs, while not optimal technologies, IoT devices can be powered more efficiently under more natural and vibrant LEDs than under their low CRI counterparts. The opposite trend is observed for IPVs with bandgaps near the optimum (1.8 eV). In this case, the cell is not only overall more efficient but will perform better under illumination with 70 and 80 CRI LEDs. This, once more, highlights the potential application space for wide-bandgap solar cells as IPVs as compared to mature technologies developed for residential and commercial solar applications, and underscores that both CT and CRI should be accounted for when characterizing IPVs with white-light LEDs.

In conclusion, while prior work has emphasized CT as the dominant factor affecting IPV bandgap energy and efficiency, we here demonstrate that both CT and CRI need to

be accounted for as the broader irradiance spectra of high-CRI LEDs shift the optimum bandgap energies to significantly lower values while also slightly reducing the maximum theoretical efficiency. We show that the choice of white-light LEDs should be carefully considered when designing and deploying IPVs, and that IPVs with bandgaps of ~ 1.72 to ~ 1.8 eV should be employed in high-CRI environments whereas IPVs with bandgaps of ~ 1.76 to ~ 1.92 eV should be employed in lower-CRI environments. Furthermore, we confirm previous notions that next-generation wide-bandgap materials should offer superior efficiency under typical indoor lighting scenarios, and we highlight that mature technologies (such as c-Si and CdTe) benefit from illumination with high-CRI light. Our work underscores the importance of accounting for both CT and CRI when developing and characterizing IPVs. These insights can guide IPV deployment in real-world environments such as smart homes, retail, or industrial monitoring, where lighting choices may vary significantly.

ACKNOWLEDGEMENTS

A.S. and J.A.R. would like to thank the Undergraduate Summer Research Program (UGSRP), NYU Tandon School of Engineering for their support. J.A.R. would like to thank Dr. Steven J. Byrnes for writing the foundational code (available at <https://sjbyrnes.com/>) that was modified for the present study.

REFERENCES

- ¹ I. Mathews, S.N. Kantareddy, T. Buonassisi, and I.M. Peters, “Technology and Market Perspective for Indoor Photovoltaic Cells,” *Joule* **3**(6), 1415–1426 (2019).
- ² G.K. Grandhi, G. Koutsourakis, J.C. Blakesley, F. De Rossi, F. Brunetti, S. Öz, A. Sinicropi, M.L. Parisi, T.M. Brown, M.J. Carnie, R.L.Z. Hoye, and P. Vivo, “Promises and challenges of indoor photovoltaics,” *Nat. Rev. Clean Technol.* **1**(2), 132–147 (2025).
- ³ D. Müller, E. Jiang, P. Rivas-Lazaro, C. Baretzky, G. Loukeris, S. Bogati, S. Paetel, S.J.C. Irvine, O. Oklobia, S. Jones, D. Lamb, A. Richter, G. Siefer, D. Lackner, H. Helmers, C. Teixeira, D. Forgács, M. Freitag, D. Bradford, Z. Shen, B. Zimmermann, and U. Würfel, “Indoor Photovoltaics for the Internet-of-Things – A Comparison of State-of-the-Art Devices from Different Photovoltaic Technologies,” *ACS Appl. Energy Mater.* **6**(20), 10404–10414 (2023).
- ⁴ W. Shockley, and H.J. Queisser, “Detailed Balance Limit of Efficiency of p - n Junction Solar Cells,” *Journal of Applied Physics* **32**(3), 510–519 (1961).
- ⁵ X. Ru, M. Yang, S. Yin, Y. Wang, C. Hong, F. Peng, Y. Yuan, C. Sun, C. Xue, M. Qu, J. Wang, J. Lu, L. Fang, H. Deng, T. Xie, S. (Frank) Liu, Z. Li, and X. Xu, “Silicon heterojunction solar cells achieving 26.6% efficiency on commercial-size p -type silicon wafer,” *Joule* **8**(4), 1092–1104 (2024).
- ⁶ M. Freunek, M. Freunek, and L.M. Reindl, “Maximum efficiencies of indoor photovoltaic devices,” *IEEE J. Photovoltaics* **3**(1), 59–64 (2013).

- ⁷ J.K.W. Ho, H. Yin, and S.K. So, "From 33% to 57% – an elevated potential of efficiency limit for indoor photovoltaics," *J. Mater. Chem. A* **8**(4), 1717–1723 (2020).
- ⁸ K.-L. Wang, Y.-H. Zhou, Y.-H. Lou, and Z.-K. Wang, "Perovskite indoor photovoltaics: opportunity and challenges," *Chem. Sci.* **12**(36), 11936–11954 (2021).
- ⁹ Q. Ma, Y. Wang, L. Liu, P. Yang, W. He, X. Zhang, J. Zheng, M. Ma, M. Wan, Y. Yang, C. Zhang, T. Mahmoudi, S. Wu, C. Liu, Y.-B. Hahn, and Y. Mai, "One-step dual-additive passivated wide-bandgap perovskites to realize 44.72%-efficient indoor photovoltaics," *Energy Environ. Sci.* **17**(5), 1637–1644 (2024).
- ¹⁰ X. Hou, Y. Wang, H.K.H. Lee, R. Datt, N. Uslar Miano, D. Yan, M. Li, F. Zhu, B. Hou, W.C. Tsoi, and Z. Li, "Indoor application of emerging photovoltaics—progress, challenges and perspectives," *J. Mater. Chem. A* **8**(41), 21503–21525 (2020).
- ¹¹ L.K. Ma, Y. Chen, P.C.Y. Chow, G. Zhang, J. Huang, C. Ma, J. Zhang, H. Yin, A.M.H. Cheung, K.S. Wong, S.K. So, and H. Yan, "High-Efficiency Indoor Organic Photovoltaics with a Band-Aligned Interlayer," *Joule* **4**(7), 1486–1500 (2020).
- ¹² H. Michaels, M. Rinderle, R. Freitag, I. Benesperi, T. Edvinsson, R. Socher, A. Gagliardi, and M. Freitag, "Dye-sensitized solar cells under ambient light powering machine learning: towards autonomous smart sensors for the internet of things," *Chem. Sci.* **11**(11), 2895–2906 (2020).
- ¹³ H. Michaels, M. Rinderle, I. Benesperi, R. Freitag, A. Gagliardi, and M. Freitag, "Emerging indoor photovoltaics for self-powered and self-aware IoT towards sustainable energy management," *Chem. Sci.* **14**(20), 5350–5360 (2023).
- ¹⁴ C. Zheng, Q. Wu, S. Guo, W. Huang, Q. Xiao, and W. Xiao, "The correlation between limiting efficiency of indoor photovoltaics and spectral characteristics of multi-color white LED sources," *J. Phys. D: Appl. Phys.* **54**(31), 315503 (2021).

SUPPLEMENTARY MATERIAL

On the Role of Color Temperature and Color Rendering Index of White-Light LEDs on the Theoretical Efficiency Limit of Indoor Photovoltaics

Aditi Sharma¹, Alexander A. Guaman¹, Jason A. Röhr^{1,*}

¹General Engineering, Tandon School of Engineering, New York University, Brooklyn, 11201 New York, United States of America

White-light LED irradiance spectra

All irradiance data were plot digitized from publicly available datasheets obtained directly from the suppliers' websites (links provided in captions below). We used the online plotdigitizer tool, plotdigitizer (<https://plotdigitizer.com/app>). While care was taken, the authors acknowledge that errors could have been introduced during the digitizing process; however, we anticipate these to be minor and not significantly affecting the calculation results presented herein.

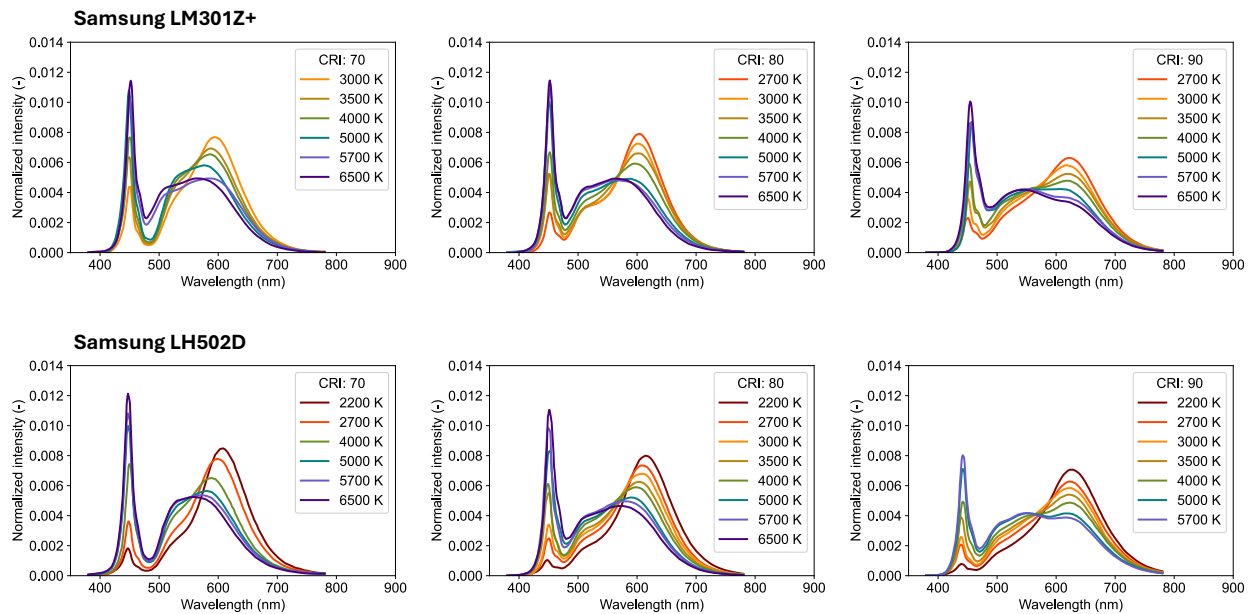


Figure S5 – Normalized irradiance spectra of Samsung LM301Z+ ([link](#)) and LH502D ([link](#)) white-light LEDs.

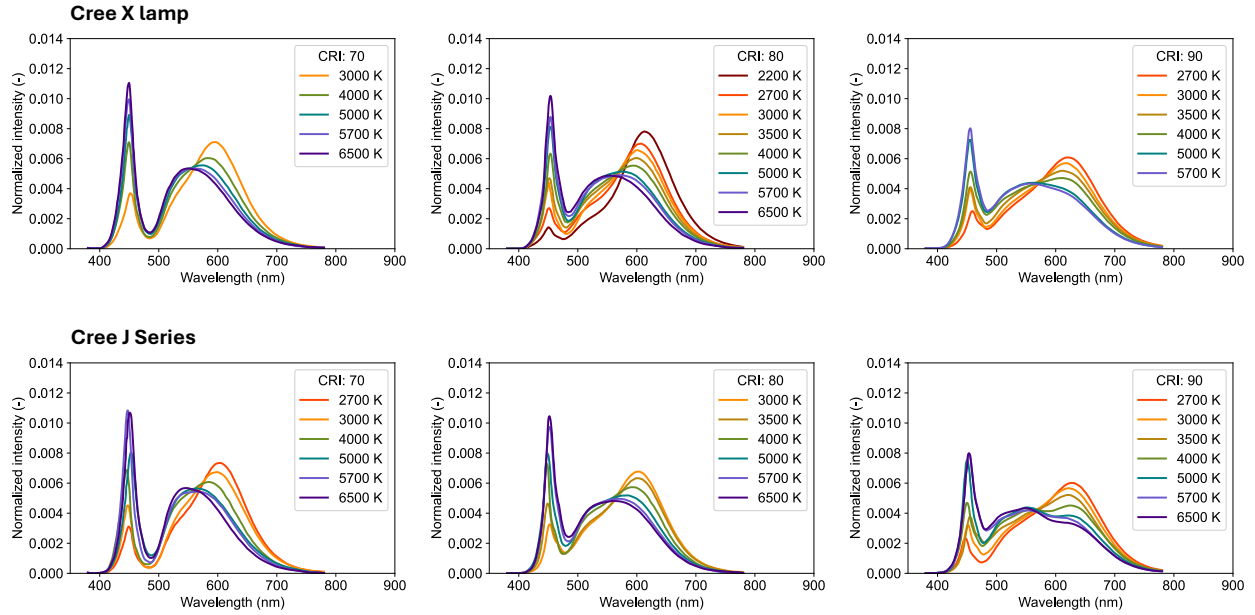


Figure S6 - Normalized irradiance spectra of Cree X Lamp ([link](#)) and J Series ([link](#)) white-light LEDs.

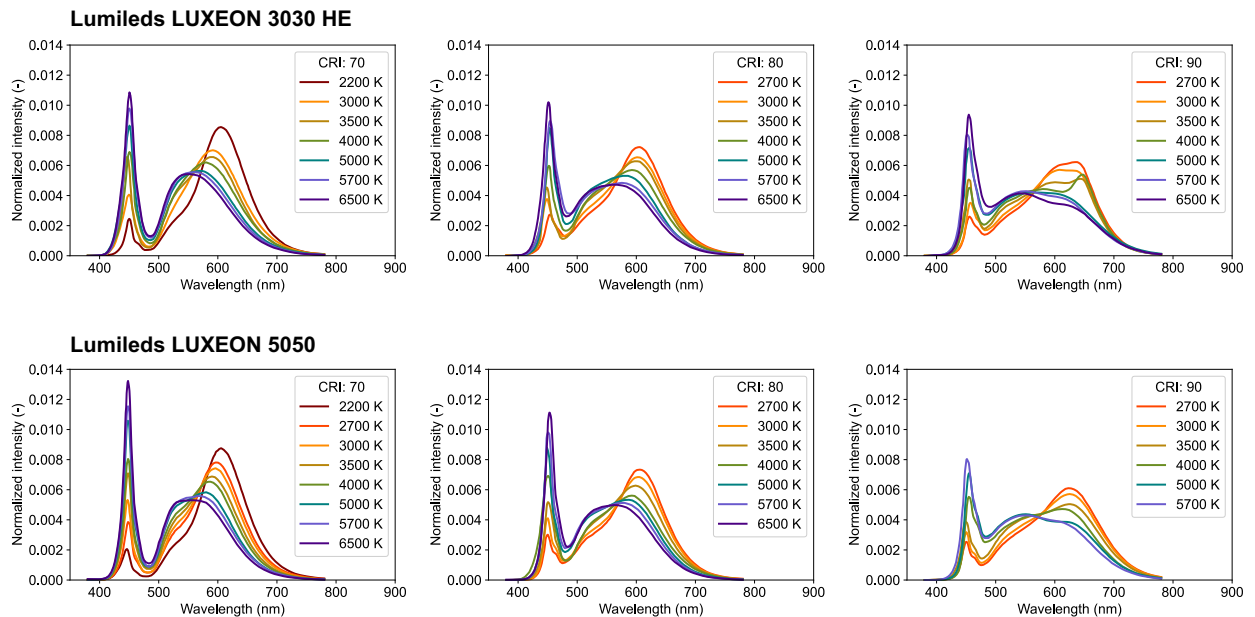


Figure S3 - Normalized irradiance spectra of Lumileds LUXEON 3030 HE ([link](#)) and 5050 ([link](#)) white-light LEDs.